Microfluidic System for Studying the Interaction of Nanoparticles and Microparticles with Cells

Omid C. Farokhzad,[*,†,‡,§] Ali Khademhosseini,[†,§,∥] Sangyong Jon,[⊥,#] Aurelia Hermmann,[⊥,¶] Jianjun Cheng,[⊥] Curtis Chin,[⊥] Alice Kiselyuk,[⊥] Benjamin Teply,[⊥] George Eng,[⊥] and Robert Langer[*,§,∥,⊥,∞]

Department of Anesthesiology, Brigham and Women's Hospital and Harvard Medical School, Boston, Massachusetts 02115, and Division of Health Sciences and Technology, Division of Biological Engineering, Department of Chemical Engineering, and Center for Cancer Research, Massachusetts Institute of Technology, Cambridge, Massachusetts 02139

Nanoparticles and microparticles have many potential biomedical applications ranging from imaging to drug delivery. Therefore, in vitro systems that can analyze and optimize the interaction of such particles with cells may be beneficial. Here, we report a microfluidic system that can be used to study these interactions. As a model system, we evaluated the interaction of polymeric nanoparticles and microparticles and similar particles conjugated to aptamers that recognize the transmembrane prostate specific membrane antigen (PSMA), with cells seeded in microchannels. The binding of particles to cells that expressed or did not express the PSMA (LNCaP or PC3, respectively) were evaluated with respect to changes in fluid shear stress, PSMA expression on target cells, and particle size. Nanoparticle−aptamer bioconjugates selectively adhered to LNCaP but not PC3 cells at static and low shear (<1 dyn/cm^2) but not higher shear (~4.5 dyn/cm^2) conditions. Control nanoparticles and microparticles lacking aptamers and microparticle−aptamer bioconjugates did not adhere to LNCaP cells, even under very low shear conditions (~0.28 dyn/cm^2). These results demonstrate that the interaction of particles with cells can be studied under controlled conditions, which may aid in the engineering of desired particle characteristics. The scalability, low cost, reproducibility, and high-throughput capability of this technology is potentially beneficial to examining and optimizing a wide array of cell−particle systems prior to in vivo experiments.

Micro- and nanoparticles are becoming increasingly important tools for a variety of biomedical applications, such as diagnostics (i.e. imaging[1−3]) and therapeutics (i.e. drug delivery[4]). These particles have been developed from a variety of materials that could be degradable or stable and have been surface modified to interact with antigens that are differentially expressed by a subset of cells or tissues, thus engineering them for targeted delivery in a specific manner. For example, by developing drug encapsulated nanoparticles from controlled release polymer systems and targeting the delivery of these vehicles to diseased cells, it may possible to maximize the therapeutic efficacy and reduce the effect of drugs.[5,6] This is particularly important when treating conditions such as cancer, where it is desired to deliver cytotoxic drugs to cancer cells while minimizing injury to nearby cells and tissues.[7] In addition, quantum dots (semiconductor nanocrystals) with tunable fluorescence have been used as highly sensitive and specific probes for in vivo cancer imaging.[1−3]

Central to the use of particles for various applications is the optimization of parameters that influence cell−particle interactions. These parameters include the size, morphology, and chemical structure of vehicles and the presence and density of escort molecules on vehicle surface, which direct the targeted delivery. Currently, a common approach is to perform sequential changes in vehicle design that affect each parameter and evaluate the consequence of each change on biodistribution of particles using in vivo animal experiments. These studies may require a large number of experimental animals, in addition to being costly and time-consuming, and may result in limiting the number of parameters that can be optimized and examined. Therefore, the development of in vitro systems that can be used to optimize various parameters associated with cell−particle interactions may be of benefit. We hypothesized that microscale devices can be used as a model of microcirculation to examine the targeting efficacy of polymeric nanoparticle and microparticle delivery vehicles in vitro. Microfluidic devices have been used to study erythrocyte deformation,[8−11] endothelial function,[12−14] leukocyte transendothelial migration,[15] neutrophil chemotaxis,[16] neuronal

* Corresponding authors. R.L.: phone, 617-253-3107; e-mail, rlanger@mit.edu. O.C.F.: phone, 617-732-6093; e-mail: ofarokhzad@partners.org.

† Authors contributed equally.

‡ Brigham and Women's Hospital and Harvard Medical School.

§ Division of Health Sciences and Technology, Massachusetts Institute of Technology.

∥ Division of Biological Engineering, Massachusetts Institute of Technology.

⊥ Department of Chemical Engineering, Massachusetts Institute of Technology.

Current address: Department of Life Science, Gwangju Institute of Science & Technology, Gwangju, South Korea.

¶ Current address: Central Institute for Medical Technology, Technical University of Munich, Bolzmannstrasse 11, 85748 Garching, Germany.

∞ Center for Cancer Research, Massachusetts Institute of Technology.

(1) Jain, R. K.; Stroh, M. *Nat. Biotechnol.* **2004**, *22*, 959−960.
(2) Gao, X.; Cui, Y.; Levenson, R. M.; Chung, L. W.; Nie, S. *Nat. Biotechnol.* **2004**, *22*, 969−976.
(3) Kim, S.; Lim, Y. T.; Soltesz, E. G.; De Grand, A. M.; Lee, J.; Nakayama, A.; Parker, J. A.; Mihaljevic, T.; Laurence, R. G.; Dor, D. M.; Cohn, L. H.; Bawendi, M. G.; Frangioni, J. V. *Nat. Biotechnol.* **2004**, *22*, 93−97.
(4) Farokhzad, O. C.; Jon, S.; Khademhosseini, A.; Tran, T. N.; LaVan, D.; Langer, R. *Cancer Res.* **2004**, *64*, 7668−7672.
(5) Langer, R. *Science* **2001**, *293*, 58−59.
(6) Langer, R. *Nature* **1998**, *392*, 5−10.
(7) Moses, M. A.; Brem, H.; Langer, R. *Cancer Cell* **2003**, *4*, 337−341.

10.1021/ac050312q CCC: $30.25
Published on Web 00/00/0000

development[17] as well as to fabricate vascularized tissue engineered constructs,[18,19] and miniaturized bioreactors.[20−23] Previously, in vitro methods have been described to test the efficacy of targeted delivery vehicles in macroscopic chambers, but these have lacked the control and the geometric scales representative of the biological microvasculature.[24,25]

Here, we used microfluidic channels lined with cells as a tool for studying parameters that effect the interaction of particles with cells in a controlled microenvironment. As a model system we studied the interaction of targeted polymeric nanoparticles and microparticles[5] with two prostate cell lines that differ in their expression of the transmembrane prostate specific membrane antigen (PSMA) protein. These particles were based on our recently reported targeted drug delivery system comprised of pegylated poly(lactic acid) (PLA) nanoparticles or microparticles conjugated to aptamers that recognize the PSMA protein.[4] PSMA is a well-known tumor antigen expressed on the surface of prostate cancer epithelial cells[26−28] and on the microvasculature of most studied tumors.[29,30] As such, PSMA is more than a prostate tumor marker, and vehicles that target this protein may have a broader utility in cancer therapy.

To test the device, microchannels were seeded with prostate cancer epithelial cells LNCaP or PC3 as model PSMA expressing or nonexpressing cell lines, respectively. The binding of particle−aptamer bioconjugates comprised of pegylated PLA particles conjugated to the A10 PSMA aptamer,[31] with these cells were evaluated with respect to changes in shear stress, the presence or absence of PSMA on target cell, and the particle size. The data indicate that nanoparticle−aptamer bioconjugates adhere to LNCaP cells but not to PC3 cells under various flow rates. In contrast, non-targeted nanoparticles or microparticles failed to demonstrate any significant binding to LNCaP or PC3 cells under any flow rate. We believe that similar systems may be used for a more comprehensive in vitro characterization and optimization of cell−particle interactions in order to potentially optimize and engineer these systems prior to animal studies.

MATERIALS AND METHODS

Materials. All chemicals were purchased from Sigma-Aldrich, unless otherwise indicated. Tissue culture medium and serum were purchased from Gibco Invitrogen Corp. Prostate epithelial cell lines, LNCaP (CRL-1740) and PC3 (CRL-1435), were purchased from ATCC. Pegylated PLA with terminal carboxylic acid functional group (PLA−PEG−COOH) was synthesized by ring-opening polymerization as described previously.[4] Poly(ethylene glycol) with terminal carboxylic acid and hydroxyl functional groups (COOH−PEG_{3400}−OH) was custom-synthesized by Nektar Therapeutics.

Synthesis of PLA−PEG−COOH. The D,L-lactide and OH−PEG_{3400}−COOH were used to synthesize poly(D,L-lactic acid)-*block*-poly(ethylene glycol)−COOH copolymer (PLA−PEG−COOH) by ring-opening polymerization. The PLA−PEG_{3400}−COOH was characterized: ^{1}H NMR (400 MHz), δ = 5.28−5.11 (br, −OC−$CH(CH_3)$O− in PLA), 3.62 (s, −CH_2CH_2O− in PEG), 1.57−1.45 (br, −OC−$CHCH_3$O− in PLA); molecular weight (GPC) M_n = 10 500 with M_w/M_n = 1.54 relative to monodispersed polystyrene standards.

Nanoparticles and Microparticles. Drug-encapsulated nanoparticles and microparticles were prepared using the water-in-oil-in-water (W/O/W) solvent evaporation procedure (double emulsion method) as described previously.[4] The size (nm) and surface charge (ζ-potential in mV) of nanoparticles were evaluated by quasielastic laser light scattering (QELS) using a ZetaPALS dynamic light scattering detector (Brookhaven Instruments Corp., 15 mW laser, incident beam = 676 nm). Surface morphology and size was also determined by high-resolution scanning electron microscopy (JEOL 6320FV).

Nanoparticle−Aptamer and Microparticle−Aptamer Conjugation.[4] Approximately 50 μL of PLA−PEG−COOH nanoparticle or microparticle suspension (~10 μg/μL in DNase- and RNase-free water) was incubated with 200 μL of 400 mM 1-(3-dimethylaminopropyl)-3-ethylcarbodimide hydrochloride (EDC) and 200 μL of 100 mM *N*-hydroxysuccinimide (NHS) in DNase- and RNase-free water for 15 min at room temperature with gentle stirring. The resulting NHS-activated particles were covalently linked to 50 μL of 5′-NH_2-modified A10 PSMA aptamers[31] (1 μg/μL in DNase/RNase-free water). The resulting aptamer−nanoparticle bioconjugates were washed, resuspended in DNase- and RNase-free water, and preserved in suspension for up to 24 h at 4 °C.

Cell Culture. The prostate LNCaP and PC3 cell lines were cultured in RPMI-1640 and Ham's F12K medium, respectively, supplemented with 100 U/mL aqueous penicillin G, 100 μg/mL

(8) Shevkoplyas, S. S.; Gifford, S. C.; Yoshida, T.; Bitensky, M. W. *Microvasc. Res.* **2003**, *65*, 132−136.
(9) Tsukada, K.; Sekizuka, E.; Oshio, C.; Minamitani, H. *Microvasc. Res.* **2001**, *61*, 231−239.
(10) Gifford, S. C.; Frank, M. G.; Derganc, J.; Gabel, C.; Austin, R. H.; Yoshida, T.; Bitensky, M. W. *Biophys. J.* **2003**, *84*, 623−633.
(11) Derganc, J.; Frank, M. G.; Gifford, S. C.; Yoshida, T.; Gabel, C.; Austin, R. H.; Bitensky, M. W. *Biophys. J.* **2001**, *80*, 145a−145a.
(12) Gray, B. L.; Lieu, D. K.; Collins, S. D.; Smith, R. L.; Barakat, A. I. *Biomed. Microdevices* **2002**, *4*, 9−16.
(13) Frame, M. D.; Sarelius, I. H. *Microcirculation* **2000**, *7*, 419−427.
(14) Frame, M. D. S.; Chapman, G. B.; Makino, Y.; Sarelius, I. H. *Biorheology* **1998**, *35*, 245−261.
(15) Cinamon, G.; Alon, R. *J. Immunol. Methods* **2003**, *273*, 53−62.
(16) Jeon, N. L.; Baskaran, H.; Dertinger, S. K. W.; Whitesides, G. M.; Van de Water, L.; Toner, M. *Nat. Biotechnol.* **2002**, *20*, 826−830.
(17) Dertinger, S. K. W.; Jiang, X. Y.; Li, Z. Y.; Murthy, V. N.; Whitesides, G. M. *Proc. Natl. Acad. Sci. U.S.A.* **2002**, *99*, 12542−12547.
(18) Borenstein, J. T.; Terai, H.; King, K. R.; Weinberg, E. J.; Kaazempur-Mofrad, M. R.; Vacanti, J. P. *Biomed. Microdevices* **2002**, *4*, 167−175.
(19) Kaihara, S.; Borenstein, J.; Koka, R.; Lalan, S.; Ochoa, E. R.; Ravens, M.; Pien, H.; Cunningham, B.; Vacanti, J. P. *Tissue Eng* **2000**, *6*, 105−117.
(20) Khademhosseini, A.; Yeh, J.; Jon, S.; Eng, G.; Suh, K. Y.; Burdick, J. A.; Langer, R. *Lab. Chip* **2004**, *4*, 425−430.
(21) Khademhosseini, A.; Suh, K. Y.; Jon, S.; Chen, G.; Eng, G.; Yeh, J.; Langer, R. *Anal. Chem.* **2004**, *76*, 3675−3681.
(22) Leclerc, E.; Furukawa, K. S.; Miyata, F.; Sakai, Y.; Ushida, T.; Fujii, T. *Biomaterials* **2004**, *25*, 4683−4690.
(23) Leclerc, E.; Sakai, Y.; Fujii, T. *Biomed. Microdevices* **2003**, *5*, 109−114.
(24) Dickerson, J. B.; Blackwell, J. E.; Ou, J. J.; Patil, V. R.; Goetz, D. J. *Biotechnol. Bioeng.* **2001**, *73*, 500−509.
(25) Blackwell, J. E.; Dagia, N. M.; Dickerson, J. B.; Berg, E. L.; Goetz, D. J. *Ann. Biomed. Eng.* **2001**, *29*, 523−533.
(26) Israeli, R. S.; Powell, C. T.; Corr, J. G.; Fair, W. R.; Heston, W. D. *Cancer Res.* **1994**, *54*, 1807−1811.
(27) Fair, W. R.; Israeli, R. S.; Heston, W. D. *Prostate* **1997**, *32*, 140−148.
(28) Kawakami, M.; Nakayama, J. *Cancer Res.* **1997**, *57*, 2321−2324.
(29) Chang, S. S.; O'Keefe, D. S.; Bacich, D. J.; Reuter, V. E.; Heston, W. D.; Gaudin, P. B. *Clin. Cancer Res.* **1999**, *5*, 2674−2681.
(30) Chang, S. S.; Reuter, V. E.; Heston, W. D.; Gaudin, P. B. *Urology* **2001**, *57*, 801−805.
(31) Lupold, S. E.; Hicke, B. J.; Lin, Y.; Coffey, D. S. *Cancer Res.* **2002**, *62*, 4029−4033.

streptomycin, and 10% fetal bovine serum. Confluent culture flasks were passaged every 4 days. Primary cell patterns were performed with medium of the respective cell.

PDMS Mold. PDMS molds were fabricated by curing prepolymer (Sylgard 184, Essex Chemical) on silicon masters etched with SU-8 photoresist. The protruding channel patterns etched on the masters resulted in PDMS replicas with receding prototypes. To cure the PDMS prepolymer, a mixture of 10:1 silicon elastomer base to curing agent was poured on the master and placed at 70 °C for 2 h. The PDMS mold was then peeled from the silicon wafer and cleaned.

Microfluidic Device. Electrical tape (3M) was placed on either end of a glass slide, leaving a thin gap (<1 mm) along the center of the slide. The slide was then coated with 25 μg/mL fibronectin (FN) for 15 min and washed in phosphate-buffered saline (PBS) (3×). Cells were then seeded on the slide at 2×10^6 cells/mL and incubated until a confluent cellular monolayer was formed. To fabricate the final device, the PDMS mold was plasma cleaned for 90 s and the electrical tape was removed while cells were maintained under moist conditions. The PDMS mold was then aligned and clamped on top of the glass slide and connected to the syringe pump (SP200i, World Precision Instruments Inc.). The device was operated on an Axiovert 200 inverted microscope equipped with an environmental chamber operated at 37 °C and 95% air/5% CO_2 humidified air (Zeiss). Cell viability was determined using the LIVE/DEAD assay (Molecular Probes). The assay consists of sequential staining of cells with Calcein AM (green dye; live cells) and DAPI (blue dye; injured or dead cells). Cell binding studies under fluid flow conditions were performed by infusing particles (5 μg/mL) suspended in cell culture medium through microchannels under a range of flow rates (0.25, 1, 4 μL/min) for 75 min followed by infusion of medium lacking particles at the same injection rate for 75 min to wash the unbound particles. The number of particles per cell was quantified by manually counting each particle attached to 150 randomly selected cells under oil immersion 100× magnification (note that some cells did not have particles attached, and these were also used in calculating the average number of particles per cell).

Mathematical Modeling of the Shear Stress. To measure the shear stress on the cells within the channels, the following equation was used[32]

$$(\tau_s^*)_{max} = \frac{6 \times 2.95 \mu Q_{2-D}^*}{H^2}$$

Where, $(\tau_s^*)_{max}$ is the maximum shear stress on the cells, μ is the viscosity of the fluid (water = 0.01 dyn s/cm^2), Q_{2-D}^* is the flow rate per unit width in the system, and H is the height of the channel. In our channels the height of the channels was 54 μm and the width was 900 μm. This equation, which is valid for cases in which the width of the channel is much larger than the width of the cell, predicts the maximum amount of shear at the center of cells adhering to microchannel walls and thus can be used to calculate the shear force of fluid flow on an adherent cell in a microchannel. This equation describes the maximum shear on a cell, and the shear stress on the cell is highest at the "tallest" part of a adhered cell (typically the nucleus) and decreases toward the periphery of the cell.[32] Despite the positional dependence of the shear stress, the values here are a good approximation of the shear stress induced on cells within these microchannels.

(32) Gaver, D. P., 3rd; Kute, S. M. *Biophys. J.* **1998**, *75*, 721−733.

RESULTS AND DISCUSSION

Development of Nanoparticle−Aptamer and Microparticle−Aptamer Bioconjugates. Using PLA−PEG−COOH, we encapsulated rhodamine−dextran (as a model drug) and developed fluorescent pegylated PLA microparticles (1855 ± 411 nm; $N = 3$) and nanoparticles (216 ± 9 nm; $N = 3$). The presence of the hydrophilic PEG polymer on the particle surface is expected to reduce the nonspecific interaction of particles with other biomacromolecules, including cell surface antigens, while increasing the circulating half-life of particles in plasma. The strongly hydrophilic PEG polymer also facilitates the presentation of the relatively less hydrophilic carboxylic acid group on the particle surface.[4] The particles were conjugated to A10 PSMA aptamer by converting the carboxylic acid group on the particle surface to activated NHS ester and covalently attaching the particles to excess amounts of 5′ NH_3-modified A10 PSMA aptamer to yield nanoparticle−aptamer and microparticle−aptamer bioconjugates (schematically represented in Figure 1A).[4,31] The density of A10 aptamer on the surface of nanoparticles and microparticles is expected to be comparable when considering the excess amount of aptamer used in all conjugation reactions. Particles were characterized for their size, surface charge (ζ-potential), and surface morphology using dynamic light scattering detector and scanning electron microscopy, respectively, as previously described.[4]

Fabrication of Microfluidic Device. We fabricated a microfluidic device and immobilized cells inside the microchannels to study the parameters that effect cell−particle interaction. Previously, we had immobilized cells within microchannels by flowing and adhering the cells within microchannels.[21] However, this process is cumbersome and requires precise control of the rate of fluid flow in order to prevent shearing of the cells as they come in contact with surfaces of the microchannel while minimizing cell necrosis due to oxygen starvation. In this paper, we built on this work by aligning PDMS microfluidic molds on cells that had been previously patterned on a substrate. A narrow strip of cells was patterned on the substrate by covering the unwanted areas with a thin removable layer. The cells were then seeded onto the slides and adhered onto the exposed substrate. The thin covering was subsequently peeled off the glass slide and the microfluidic mold was then aligned on the channel (schematically represented in Figure 1B).

To ensure that the immobilized cells in the channels were alive and could tolerate our experimental procedure of fluid flow, we tested for cell viability using calcein AM and DAPI to determine cellular function and membrane integrity, respectively. Calcein AM is membrane permeable and thus can be introduced into cells via incubation. Once inside the cells, calcein AM is hydrolyzed by endogenous esterase into a negatively charged green fluorescent calcein, which is retained in the cytoplasm. DAPI is a blue fluorescent dye that permeates through cell membranes at a very slow rate, and therefore, during a short incubation, it would stain the nuclei of cells after loss of membrane integrity. The data demonstrates that both LNCaP and PC3 cells remained viable after

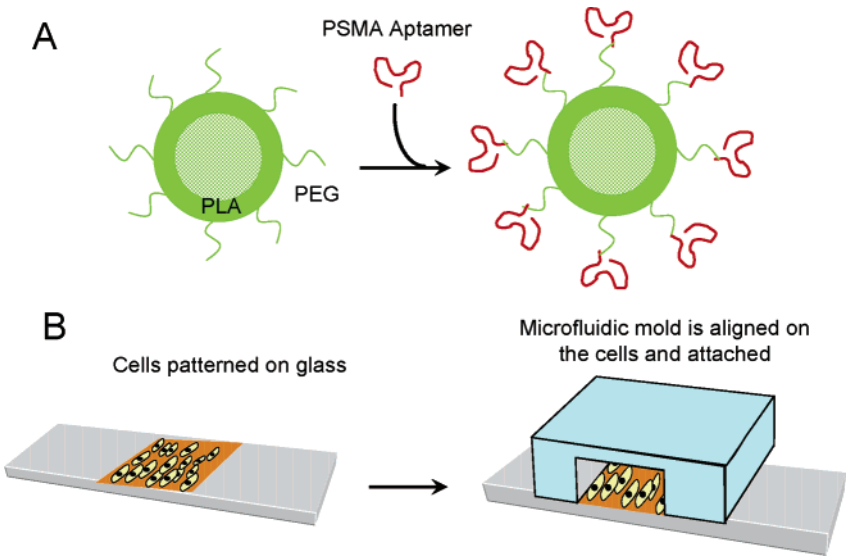

Figure 1. Schematic diagram of the nanoparticle−aptamer bioconjugate and the microfluidic device development. (A) The surface of pegylated PLA particles was modified by covalent conjugation with RNA aptamers that recognize the PSMA protein. (B) Model cell lines, LNCaP (+PSMA) or PC3 (−PSMA), which differ in the pattern of PSMA expression, were patterned on glass substrates and a microfluidic mold was aligned over the cell pattern to develop the microchannels for experimental procedures.

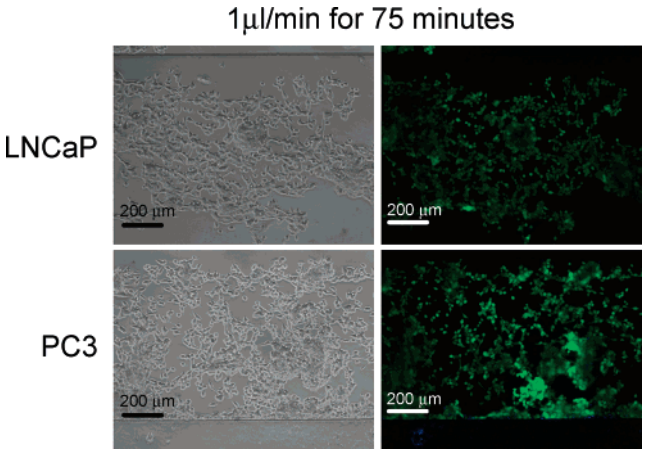

Figure 2. The viability of LNCaP (top panels) or PC3 (bottom panels) cells examined within microchannels after fluid flow at 1 μL/min for 75 min. Cells were subsequently stained with calcein AM (green) and DAPI (blue) and visualized by fluorescent microscopy. Green fluorescence signifies an intact plasma membrane and marks cell viability, while blue fluorescence signifies a compromised plasma membrane consistent with cell injury or cell death.

fluid flow for the experimental conditions tested, indicating that the process shown here can be used to generate immobilized cell layers within microchannels (>98% of cells expressed green fluorescence) (Figure 2).

Specificity of Nanoparticle−Aptamer and Microparticle−Aptamer Bioconjugates Binding under Static Fluid Conditions. We tested the binding of nanoparticle−aptamer and microparticle−aptamer bioconjugates to LNCaP and PC3 cells under static fluid conditions (Figure 3). Nanoparticle−aptamer bioconjugates and microparticle−aptamer bioconjugates, but not equivalent control particles lacking the A10 PSMA aptamer, adhered to LNCaP cells, which express the PSMA protein. Consistent with the lack of PSMA protein expression on PC3 cells, both bioconjugates and control particles failed to adhere on to the surface of PC3 cells. The high specificity of these delivery vehicles is due in part to the specific interaction of A10 PSMA aptamers on vehicle surface with their target PSMA antigen on LNCaP cells and in part due to PEG's ability to reduce nonspecific interaction with proteins present on PC3 cell membrane. Indeed, this combination results in targeted delivery vehicles with remarkably low nonspecific binding characteristics.

Nanoparticle−Aptamer and Microparticle−Aptamer Bioconjugate Binding under Flow Conditions. We next studied the effect of shear stress generated by fluid flow through microchannels on adhesion of nanoparticle or nanoparticle−aptamer bioconjugates to LNCaP and PC3 cells. Specifically, we were interested to see the effects of the following parameters on targeting efficacy of nanoparticle drug delivery vehicles: (1) the presence or absence of PSMA on target cells, (2) the presence or absence of aptamer on vehicle's surface, and (3) the rate of fluid flow (corresponding to shear stress). In each experiment, nanoparticle−aptamer bioconjugates or control nanoparticles lacking the A10 PSMA aptamers (5 μg/mL) were injected in the channels at 0.25, 1, or 4 μL/min to examine the shear values that result in loss of particle−cell interaction. The maximum shear stress values for 0.25, 1, and 4 μL/min flow rates were calculated to be 0.28, 1.1, and 4.5 dyn/cm^2 (see Materials and Methods), respectively, which are in the lower range of shear stresses present at different regions of systemic microvasculature.[15,33−36] Each nanoparticle group was first injected in microchannels at the desired speed for 75 min followed by 75 min of wash at the same injection rate prior to imaging of cells by transmission light and fluorescent microscopy. Nanoparticle and nanoparticle−aptamer bioconjugate adhesion to LNCaP and PC3 cells was

(33) Taylor, C. A.; Cheng, C. P.; Espinosa, L. A.; Tang, B. T.; Parker, D.; Herfkens, R. J. *Ann. Biomed. Eng.* **2002**, *30*, 402−408.
(34) Moore, J. E.; Xu, C. P.; Glagov, S.; Zarins, C. K.; Ku, D. N. *Atherosclerosis* **1994**, *110*, 225−240.
(35) Masuda, M.; Fujiwara, K. *Front Med. Biol. Eng.* **1993**, *5*, 79−87.
(36) Wang, D. M.; Tarbell, J. M. *J. Biomech. Eng.* **1995**, *117*, 358−363.

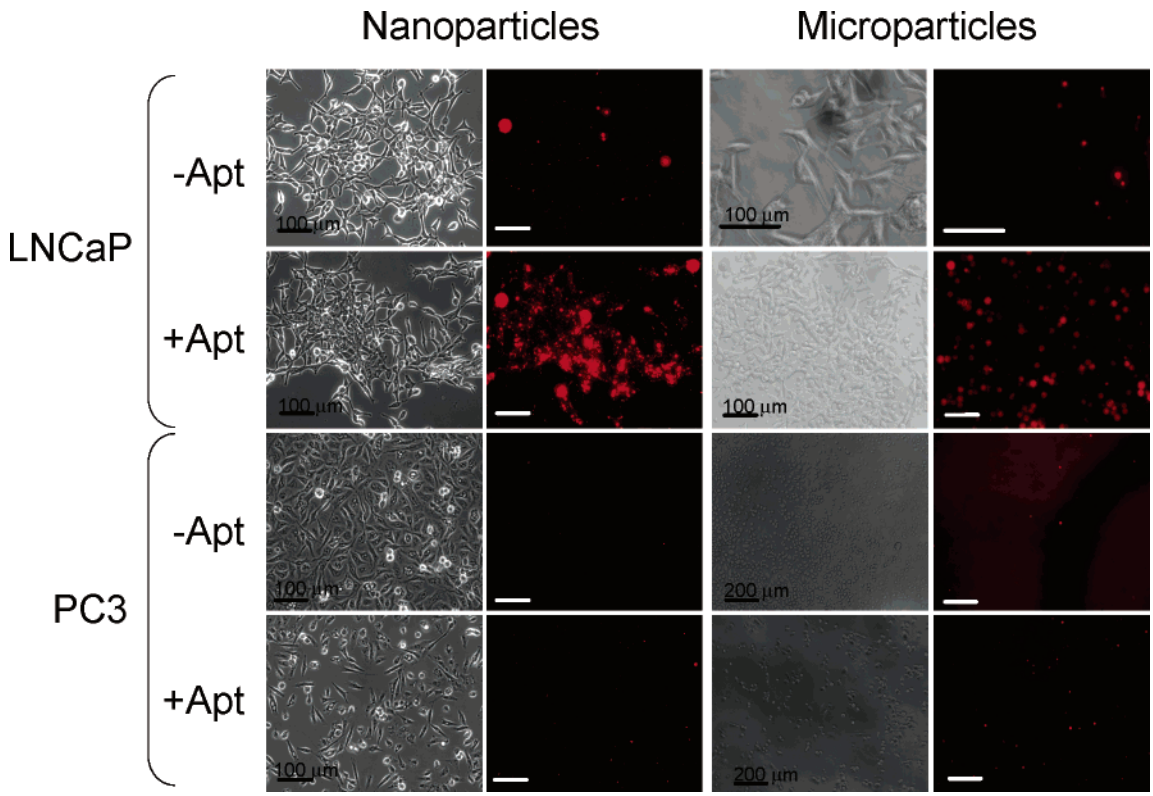

Figure 3. The binding of rhodamine-labeled dextran encapsulated nanoparticles (left two columns) and microparticles (right two columns), or similar particles conjugated to the PSMA aptamer, with LNCaP and PC3 cells was evaluated under static fluid conditions. The particles are visualized by red fluorescence.

quantified by manually counting the number of particles attached per cell ($N = 150$ cells) under high magnification (Figure 4). In addition, calcein AM/DAPI staining was performed with each experiment to confirm cell viability under these conditions.

The combined presence of PSMA antigen on cell surface and the A10 PSMA aptamer on nanoparticles significantly enhanced cellular binding of vehicles as predicted. This is important, since targeted drug delivery vehicles should exhibit minimal binding characteristic toward non-targeted cells while exhibiting an enhanced binding characteristic toward the targeted cells. Furthermore, changes in flow rate corresponding to an increasing amount of shear stress adversely affect binding of nanoparticle−aptamer bioconjugate with cells. Figure 4 shows fluorescent images of the LNCaP cells after the attachment of the nanoparticle−aptamer bioconjugates under various shear stress values. At low shear stress (i.e. <1.1 dyn/cm^2), the average number of attached nanoparticle−aptamer bioconjugate was >10 per cell. However, when the bioconjugate was injected in channels at 4 μL/min, corresponding to shear stress of 4.5 dyn/cm^2, there was a significant decrease in attachment of the particles ($p < 0.05$). In addition, it was found that the particles did not adhere to PC3 cells, irrespective of the flow conditions, indicating that the presence of the PSMA protein was essential for the observed binding. Furthermore, the lack of adhesion of control nanoparticles to LNCaP cells further illustrates the specific targeting of nanoparticle−aptamer bioconjugates to PSMA expressing cells.

We next examined the effect of particle size on vehicle's targeting efficiency using microparticles with mean diameter ~8.6-fold larger than that of the nanoparticles. We evaluated the binding characteristics of microparticle−aptamer bioconjugates and control microparticles lacking the A10 PSMA aptamer to LNCaP and PC3 cells under different shear stress conditions. Despite the selective adhesion of the microparticle−aptamer bioconjugates to LNCaP cells under static conditions, these bioconjugates did not adhere to LNCaP cells at any of the experimentally tested shear stresses (Figure 5). This lack of adhesion is potentially due to the imbalance between the drag forces exerted on the microparticles (i.e., shear forces by the flowing fluid) and the binding interaction between the A10 PSMA aptamer on microparticle surface and the PSMA protein on LNCaP plasma membrane. The size of the particle will greatly influence the drag force, gravity, and the surface area of the particles. In general, the forces attaching the particles to the surface of the targeted cell (i.e. ligand−receptor interactions) should be larger than forces pulling away the particle (i.e. drag force from the fluid). Our data suggest that, as the particle size increases, the fluid drag forces increase at a greater pace in comparison to the forces mediated by the affinity of aptamer for its target antigen. We had also previously shown that nanoparticle−aptamer bioconjugates are taken up by LNCaP cells after binding to cell surface and thus may be less affected by fluid drag forces as compared to microparticle−aptamer bioconjugates. Therefore, in this experimental system the nanoparticles provide a more suitable targeted delivery vehicle in comparison to the microparticles. Although not examined, similar microfluidic systems can be used to determine the optimal surface concentration of a targeting molecule on delivery vehicles prior to in vivo evaluation. For example, by increasing the density of aptamers on microparticle surface, it may be possible to obtain specific binding of these vehicles under the desired shear stress conditions. This problem is confounded by the fact that, by

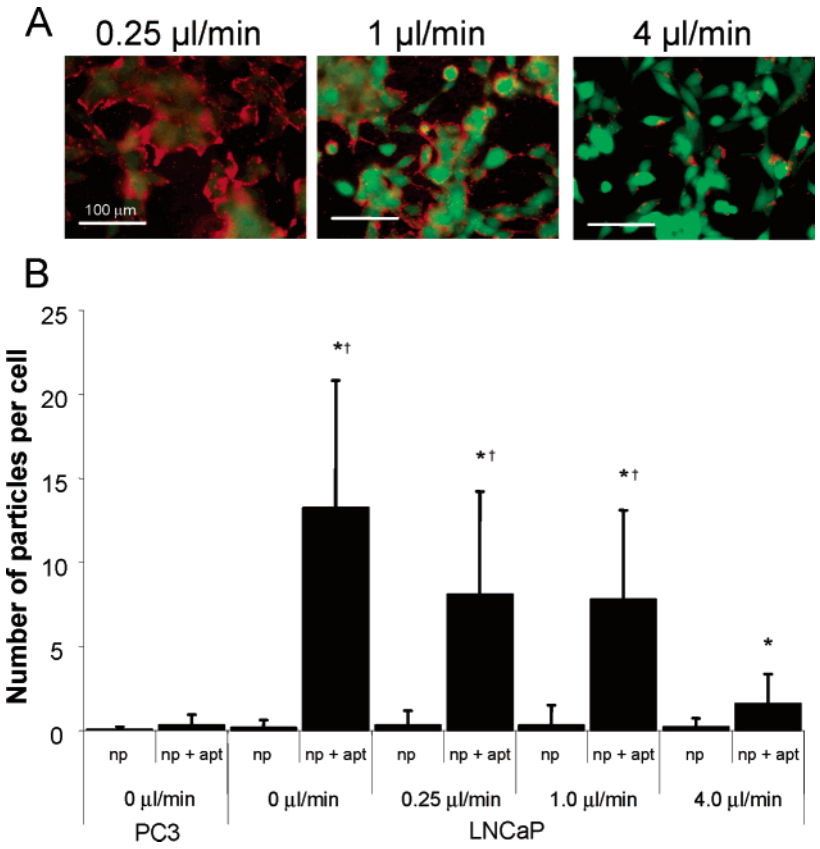

Figure 4. Effect of fluid shear on nanoparticle or nanoparticle−aptamer bioconjugate adhesion to cells. (A) The fluorescent images of rhodamine-labeled dextran-encapsulated nanoparticle−aptamer bioconjugates binding to LNCaP cells under fluid flow at 0.25, 1, or 4 μL/min. The cell viability was determined by staining with calcein AM (green) and DAPI (blue), and the nanoparticle−aptamer bioconjugates are shown in red. (B). The number of nanoparticle (np) or nanoparticle−aptamer bioconjugate (np + apt) attachment to LNCaP or PC3 cells was quantified under static or fluid flow conditions by manually counting the number of particles per cell under oil immersion (100× magnification) ($N = 150$ randomly selected cells per group; note that some cells did not have particles attached and these were also used in calculating the average number of particles per cell). An asterisk represents a statistically significant difference between nanoparticle and nanoparticle−aptamer bioconjugate groups ($p < 0.05$). A dagger represents a significant difference relative to the 4 μL/min group ($p < 0.05$). Red fluorescence indicates rhodamine-labeled dextran-encapsulated particles.

increasing the density of aptamers on particle surface, it is possible to adversely affect the aptamer binding characteristic through spatial hindrance caused by the proximity of aptamers (Farokhzad, O. C.; Jon, S.; Khademhosseini, A.; Langer, R. Unpublished observation). This hypothetical issue underscores the importance of in vitro systems for optimizing targeted delivery vehicles prior to further in vivo evaluation.

It should be noted that we used cell culture medium (low viscosity Newtonian fluid) as a substitute for blood (high viscosity non-Newtonian fluid) in all of our binding studies with nanoparticles and microparticles. This approach is in general valid because the expectation is that the same Reynolds number would give the same rheological behavior, regardless of the viscosity of the fluid. Thus, by altering the fluid flow rate, we corrected for the differences in fluid viscosity between blood and cell culture medium and tested the binding of particles under equivalent fluid shear stress. There is, however, intrinsic differences between cell culture medium and blood that limits the translation of these data to what may be observed in vivo. One such difference is the influence of circulating cells (~45% of blood volume) as well as plasma proteins on bioconjugate behavior in vivo. For example, circulating cells may alter particle settling on target cells while plasma proteins may interact with particle surface affecting its ligand binding properties and target antigen recognition.

A potential drawback of an in vitro system to study targeted drug delivery is the differences in the biology of targeted and non-targeted cells in vitro vs in vivo. For example, it is well known that shear stress induces changes in gene expression and cell shape of various cell types.[37,38] Consequently, these changes may have altered the expression of the PSMA antigen on LNCaP cell surface at high shear values and qualitatively affect the interpretation of our data. However, since alteration in gene and protein expression are slower in onset than the durations used in our experiments,[12,39] it is unlikely that the PSMA antigen expression was significantly altered as a result of fluid flow.

Another potential limitation of the current model is that the flow of particles was not pulsatile, as is the case physiologically arteries in systemic vasculature. We anticipate that the addition of time-varying pulsatile flow could enhance this system in order to better mimic the physiological flow in systemic vasculature. Furthermore, other parameters that influence the interaction of particles with cells that have not been specifically addressed in this device may include the clogging of microvasculature particles and the blood cells' interactions with the particles. These complex

(37) Resnick, N.; Gimbrone, M. A., Jr. *FASEB J* **1995**, *9*, 874−882.
(38) Wasserman, S. M.; Topper, J. N. *Vasc. Med.* **2004**, *9*, 35−45.
(39) Fisher, A. B.; Chien, S.; Barakat, A. I.; Nerem, R. M. *Am. J. Physiol. Lung Cell Mol. Physiol.* **2001**, *281*, L529−533.

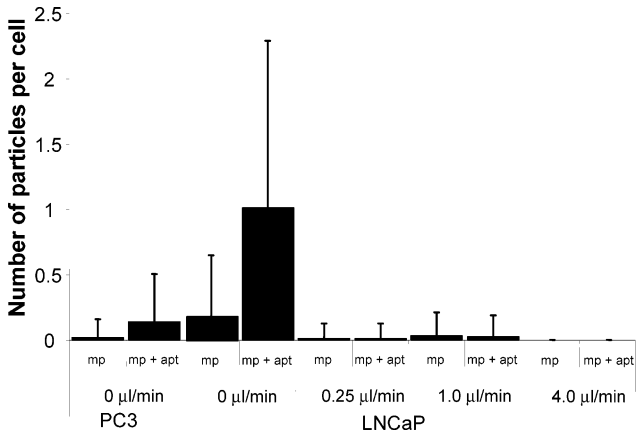

Figure 5. Effect of fluid shear on microparticle (mp) or microparticle−aptamer bioconjugate (mp + apt) adhesion to LNCaP or PC3 cells under 0, 0.25, 1, or 4 μL/min fluid flow rate were determined. The number of microparticle or microparticle−aptamer bioconjugate attachment to LNCaP or PC3 cells was quantified under static or fluid flow conditions by manually counting the number of particles per cell under oil immersion (100× magnification) ($N = 150$ randomly selected cells per group; note that most cells did not have particles attached and these were also used in calculating the average number of particles per cell; consequently, the average number of particles per cell may be less than 1). Red fluorescence indicates rhodamine-labeled dextran-encapsulated particles.

parameters may be modeled in future systems that integrate some of these complexities. However, it is clear that these devices will be useful with respect to optimizing particular parameters of nanoparticles for various applications that may aid in reducing the development time and lead to improved delivery vehicles.

CONCLUSION

In summary, we have developed a microfluidic model that could be used to study the interaction of particles and cells. We have used pegylated PLA nanoparticles and microparticles and studied their interaction with cells under various conditions. We demonstrated that the presence of ligands on vehicle surface, size of vehicles, and amount of shear stress generated during fluid flow can affect the targeting efficiency of these vehicles in vitro. Our studies reproducibly demonstrated that the shear stress generated from fluid flow can have a significant effect on the binding characteristic of targeted delivery vehicles in vitro. Depending on the specific application, the ideal vehicle should be able to bind to its target cell at a particular range of shear stress. Therefore, this model can be used to determine the ideal particle size and ligand density on particle surface for binding to target cells under fluid flow conditions. We postulate that similar microfluidic models can be designed to test multiple parameters simultaneously and therefore maximally optimize the physical and chemical properties of therapeutic and diagnostic particles prior to their in vivo evaluation.

ACKNOWLEDGMENT

The authors wish to thank Dr. Chris Cannizzaro for helpful discussions. This work was supported in-part by the MIT David Koch Cancer Research Fund, Draper laboratory, Institute of Solder Nanotechnology (DAAD-19-02-D-002), the Foundation for Anesthesia Education and Research, and a Kirschstein-NRSA award (T32 GM07592).

Received for review February 19, 2005. Accepted June 7, 2005.

AC050312Q